AIP | Review of Scientific Instruments

A lightweight balloon-carried cloud charge sensor

K. A. Nicoll and R. G. Harrison

Citation: Rev. Sci. Instrum. **80**, 014501 (2009); doi: 10.1063/1.3065090
View online: http://dx.doi.org/10.1063/1.3065090
View Table of Contents: http://rsi.aip.org/resource/1/RSINAK/v80/i1
Published by the American Institute of Physics.

A lightweight balloon-carried cloud charge sensor

K. A. Nicoll[a] and R. G. Harrison
Department of Meteorology, University of Reading, P.O. Box 243, Earley Gate, Reading, Berkshire RG6 6BB, United Kingdom

(Received 30 October 2008; accepted 14 December 2008; published online 9 January 2009)

Despite the importance of microphysical cloud processes on the climate system, some topics are under-explored. For example, few measurements of droplet charges in nonthunderstorm clouds exist. Balloon carried charge sensors can be used to provide new measurements. A charge sensor is described for use with meteorological balloons, which has been tested over a range of atmospheric temperatures from −60 to 20 °C, in cloudy and clear air. The rapid time response of the sensor (to $>10\ \mathrm{V\,s^{-1}}$) permits charge densities from $100\ \mathrm{fC\,m^{-3}}$ to $1\ \mathrm{nC\,m^{-3}}$ to be determined, which is sufficient for it to act as a cloud edge charge detector at weakly charged horizontal cloud boundaries. © *2009 American Institute of Physics.* [DOI: 10.1063/1.3065090]

I. INTRODUCTION

The electrical characteristics of the atmosphere are conventionally summarized by a conceptual framework known as the global atmospheric electric circuit.[1] Charge separation in thunderstorms generates a large potential difference ($\sim$300 kV) between the ionosphere and the Earth's surface. Associated with this potential difference, the finite electrical conductivity of atmospheric air permits vertical current flow in fair weather or nonthunderstorm regions. If this vertical current passes through a horizontal layer cloud, the cloud edges become electrified as a result of the appreciable conductivity change at the boundary between the clear and cloudy air.[2] The charge resides on cloud droplets and cloud particles. It is thought that highly charged droplets may influence cloud microphysical processes such as particle-droplet collection,[3,4] droplet-droplet collisions,[5] and droplet activation.[6] Few measurements of charge in nonthunderstorm clouds have been made, but 10–100 electronic charges per drop have been observed in stratiform clouds.[7,8] Charge sensors can be readily carried aloft through clouds using meteorological balloons and an inexpensive and lightweight system—the cloud edge charge detector (CECD)—is described here.

II. CLOUD EDGE CHARGE DETECTOR DESCRIPTION

The sensor comprises a sensing electrode, connected to an electrometer, miniaturizing a previous approach.[9] The electrode consists of an exposed brass sphere of diameter 12 mm, supported by tinned copper wire, connected through Polytetrafluroethylene (PTFE) sleeving to the electrometer circuit. The circuit is housed inside a shielded box with dimensions of $35\times35\times20\ \mathrm{mm^3}$. The sensor is flown on a Vaisala RS92 radiosonde, with the sensing electrode protruding $\sim$15 mm. A conceptual diagram of the sensor arrangement is shown in Fig. 1(a). Connection to the RS92 is made through a 12 bit digital acquisition system (DAS) developed from a previous system.[10] This also provides a 9 V supply, and the sensor output voltage is directly reported to and logged by the ground station, together with the meteorological parameters and location information.

The electrometer circuit is shown in Fig. 1(b). It consists of an electrometer with a reset stage, added to prevent saturation effects from strongly charged regions compromising the remainder of the flight. The ultra-low leakage reset switch utilizes a double j-FET arrangement (Q1a and Q1b), as described previously.[11] The electrometer uses a dual LMC6042 op-amp, one stage of which is configured in unit gain voltage follower mode. Two outputs are provided, ANALOG out 1 and 2, which are logged simultaneously. ANALOG out 1 is the output directly from the electrometer voltage follower. ANALOG out 2 provides more sensitivity by using an inverting amplifier stage with a gain of −10. The simultaneous recording of the two outputs allows a wide dynamic range to be measured. The reset pulse is provided by the DAS every 128 s, lasting 5 s.

III. RESPONSE AND CALIBRATION

The sensing electrode responds to changes in charge, either induced, or from impaction of charged particles. The induced effect is used for calibration here.

A. Induced current calibration

From Maxwell's equation, when an electric field $\vec{E}$ varies with time t, the current density $\vec{j}$ induced in a conductor is given by

$$\varepsilon_0 \frac{\partial \vec{E}}{\partial t} + \vec{j} = 0, \tag{1}$$

where $\varepsilon_0 = 8.85\times10^{-12}\ \mathrm{F\,m^{-1}}$. Considering only vertical (z direction) changes in the electric field and assuming no other currents flow to the electrode, the change in the electrode potential V is given by

[a]Electronic mail: k.a.nicoll@reading.ac.uk.

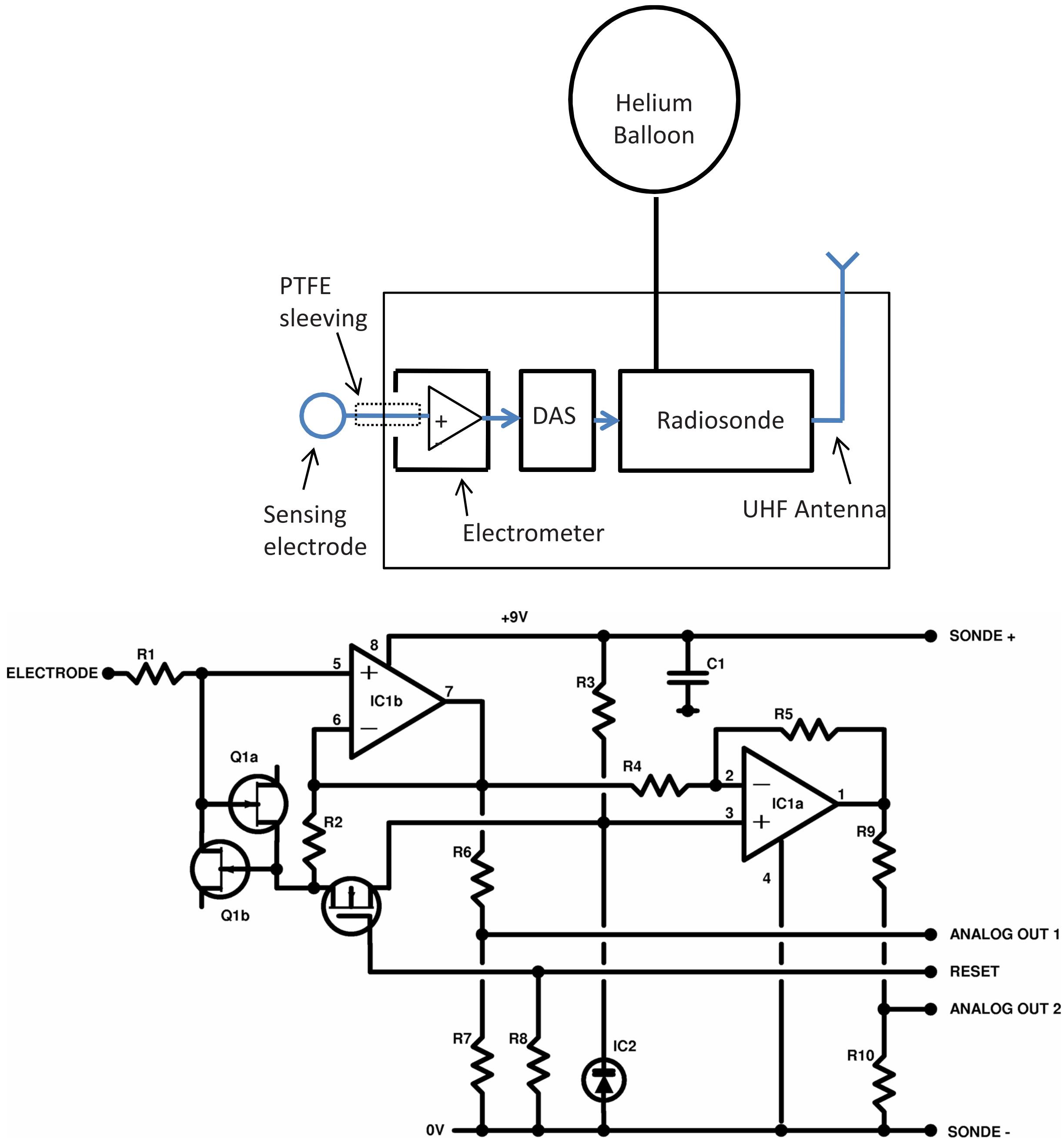

FIG. 1. (Color online) (a) Conceptual diagram of measuring system, showing the sensing electrode, electrometer, DAS, and radiosonde. (b) Electronic circuit diagram. Components: R1=1 MΩ, R2, R6, R7, R9, R10=10 kΩ, R3, R4=91 kΩ, R5=910 kΩ, R8=100 kΩ, C1=1 μF, IC1=LMC6042 (dual op-amp), IC2=ZREF-25 (2.5 V ref), Q1a,b=J113 j-FET, and Q2=VN10LP (VFET).

$$-\varepsilon_0 A_{\mathrm{eff}} \frac{dE_z}{dt} = C\frac{dV}{dt}, \tag{2}$$

where A_{eff} is the effective area through which the field acts and C is the capacitance of the electrode. It follows that, if the magnitude of the rate of change in sensor voltage is measured within a field changing at a known rate, the gradient of a graph of dE_z/dt against dV/dt is $(C/A_{\mathrm{eff}}\varepsilon_0)$, providing the geometrical factor C/A_{eff}. By denoting C/A_{eff} as $\varepsilon_0/d_{\mathrm{eff}}$ (from capacitance considerations) we get

$$\frac{dE_z}{dt} = -\frac{1}{d_{\mathrm{eff}}}\frac{dV}{dt}. \tag{3}$$

An estimate of d_{eff} was obtained experimentally using separated horizontal plates to generate a uniform electric field. A triangular voltage waveform produced by a signal generator was applied across the plates, creating a changing electric field dE_z/dt at frequencies between 10 and 40 Hz. The sensor-electrometer system was suspended vertically at the center of the two plates by a fine string. Frequency and amplitude of the applied waveform were varied and the dV/dt response of the sensor to the time varying field recorded. Figure 2 shows a graph of dE_z/dt against the magnitude of dV/dt, with dV/dt measured directly from a Fluke digital oscilloscope (model 105B). Two experiments were undertaken using different plate separations. The agreement between the two sets of measurements indicates that the separations chosen are sufficient for local distortions to be negligible. A linear least-squares fit to all points gives

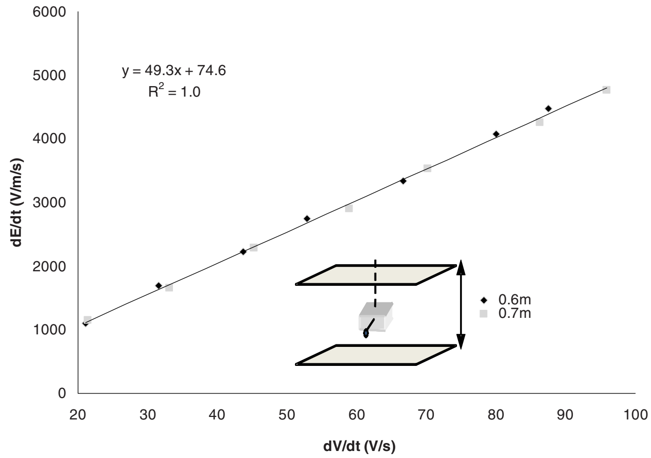

FIG. 2. (Color online) Magnitude of sensor voltage (dV/dt) against time varying vertical electric field (dE_z/dt), for two different plate separations (0.6 m black points and 0.7 m gray points). The linear least-squares fit was obtained using all points.

$1/d_{\mathrm{eff}}=49.3\ \mathrm{m}^{-1}$, i.e., $d_{\mathrm{eff}}=20.3$ mm, a factor of 1.7 greater than the physical diameter.

B. Response to atmospheric charge

During a vertical atmospheric ascent, the sensor voltage responds to induced variations associated with charge regions and, transiently, the transfer of charge with its surroundings by collision. Our observations from several ascents show that, in cloud, the collisional charge fluctuations are small, compared with the induced changes as cloud is approached. Further evidence for the sensor's operation principally through an induced effect is apparent in its behavior at heights above 10 km. At these heights the air conductivity is sufficiently large that the vertical field gradient is negligible,[12] and the sensor ceases to show appreciable changes.

For a region of atmospheric space charge ρ (the difference between the net positive and negative charge per unit volume), Gauss' law in one dimension links ρ to the vertical field gradient by

$$\rho = -\varepsilon_0 \frac{dE_z}{dz}. \tag{4}$$

The vertical gradient and temporal variations are related through the ascent rate w by

$$-\varepsilon_0 \frac{dE_z}{dz} = -\varepsilon_0 \frac{dE_z}{dt}\frac{dt}{dz} = -\varepsilon_0 \frac{dE_z}{dt}\frac{1}{w}. \tag{5}$$

By equating Eq. (5) with Eq. (3), the space charge measured by the sensor is directly related to the voltage output by

$$\rho = \frac{\varepsilon_0}{d_{eff}}\frac{1}{w}\frac{dV}{dt}. \tag{6}$$

Here w can be determined from consecutive radiosonde pressure measurements, which are made approximately every second. For the 12 bit data acquisition system and a 10 V op-amp supply voltage, with the dual channel approach, the measurable range of space charge is from 100 fC m^{-3} to 1 nC m^{-3}, assuming $w=5\ \mathrm{ms}^{-1}$ and 1 Hz sampling. (The rapid time response of the electrometer, to $>10\ \mathrm{V\,s}^{-1}$, was established in the experiment in Sec. III A.)

IV. ATMOSPHERIC RESULTS

The integrated radiosonde and CECD system was tested on a standard meteorological flight in overcast conditions. Before launch an antistatic coating was applied to the sensor system to eliminate charging associated with handling. Conditions at the surface were dry and the cloud base was determined at about 2 km from an adjacent doppler lidar. Figure 3(a) displays the temperature (black points) and relative hu-

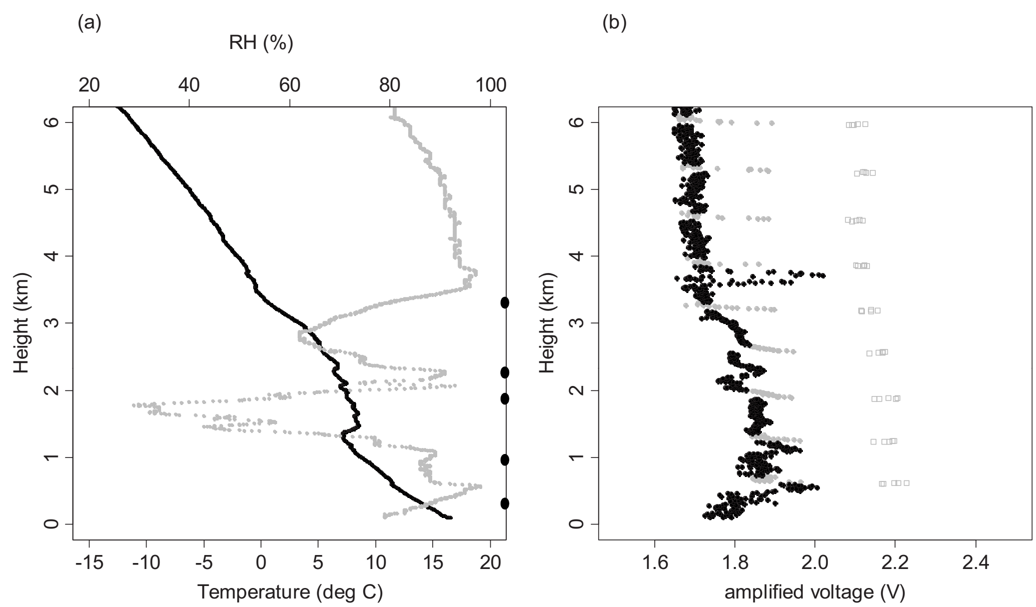

FIG. 3. Vertical profiles of (a) air temperature (black) and relative humidity (gray), with RH (cloud) boundaries marked with dots (on the right hand axis). (b) CECD voltage (black circles) and reset voltage (gray squares). Measurements determined within 20 s of the reset pulse are affected by the switch operation and have been marked by gray circles. The mean ascent rate was 5 ms^{-1}.

midity (RH) (gray points) as measured by the standard meteorological sensors flown. Multiple temperature inversions and high RH indicate several cloud layers between the surface and 4 km. Figure 3(b) shows the voltage on the sensor electrode (black circles), which is regularly interrupted by the reset switch (gray squares). As the CECD passes through the cloud, there are large variations in the sensor voltage. In the steady humidity region above 4 km, the variations decrease. These variations demonstrate the presence of charge structures in nonthunderstorm stratiform clouds. Using the calibration data and Eq. (5), the space charge in this relatively weakly charged case, chosen to illustrate the system sensitivity is, on average, $\sim 20\ \mathrm{pC\,m^{-3}}$. The calculated charge on the cloud edge at 4 km is $\sim 100\ \mathrm{pC\,m^{-3}}$.

ACKNOWLEDGMENTS

K.A.N. acknowledges a studentship from the Natural Environment Research Council (NERC) and the assistance of the technical staff in the Reading Meteorology department. The Met Office supported flights from their upper air station at Kehelland, Camborne, Cornwall, U.K.

[1] M. J. Rycroft, S. Israelsson, and C. Price, J. Atmos. Sol.-Terr. Phys. **62**, 1563 (2000).
[2] L. Zhou and B. A. Tinsley, J. Geophys. Res. **112**, D11203, DOI:10.1029/2006JD007998 (2007).
[3] B. A. Tinsley, Space Sci. Rev. **94**, 231 (2000).
[4] S. N. Tripathi and R. G. Harrison, Atmos. Res. **62**, 57 (2002).
[5] A. Khain, V. Arkhipov, M. Pinsky, Y. Feldman, and Y. Ryabov, J. Appl. Meteorol. **43**, 1513 (2004).
[6] R. G. Harrison and M. H. P. Ambaum, Proc. R. Soc. London, Ser. A **464**, 2561 (2008).
[7] K. V. Beard, H. T. Ochs, and C. H. Twohy, Geophys. Res. Lett. **31**, L14111, DOI:10.1029/2004GL020465 (2004).
[8] S. Twomey, Tellus **8**, 445 (1956).
[9] R. G. Harrison, Rev. Sci. Instrum. **72**, 2738 (2001).
[10] R. G. Harrison, Rev. Sci. Instrum. **76**, 026103 (2005).
[11] K. A. Nicoll and R. G. Harrison, Rev. Sci. Instrum. **79**, 084502 (2008).
[12] G. A. Bazilevskaya, I. G. Usoskin, E. O. Flükiger, R. G. Harrison, L. Desorgher, R. Bütikofer, M. B. Krainev, V. S. Makhmutov, Y. I. Stozhkov, A. K. Svirzhevskays, N. S. Svirzhevsky, and G. V. Kovaltsov, Space Sci. Rev. **137**, 149 (2008).